MASS TRANSFER IN ANNULAR CYLINDRICAL ELECTROCHEMICAL CELLS

Etienne Roux[1]

[1] Anglo Research, a division of Anglo Operations Ltd, Johannesburg, South Africa

ABSTRACT

Novel electrochemical cell designs are emerging as alternative process units for various applications in industry. Most of the advances in electrochemical cell design are in the field of improving mass transfer. Improved mass transfer allows increased specific production capacity, reduced footprint, increased selectivity, and plating from lower concentrations. One of the designs gaining acceptance in industry is the annular/tubular/cylindrical electrochemical cell. This paper discusses the effect of flow rates and inlet geometry on mass transfer in an annular electrochemical cell, using silver as a tracer element while plating from copper electrolyte. It is concluded that swirl flow significantly improves mass transfer over axial flow in annular electrochemical cells due to the slower formation of the diffusion layer. The noble tracer method provides be valuable tool in cell design and understanding mass transfer in annular electrochemical cells.

Keywords: Mass transfer, electrochemical cell, electrowinning, copper, silver

INTRODUCTION

Electrolytic cell design has been evolving to meet the ever changing requirements posed by industry. Most of the focus in cell development is on improving mass transfer in electrochemical cells. By improving the mass transfer in cells a host of benefits can be derived:

- Increased mass transfer increases the limiting current density. This means that electrochemical cells can operate at higher current densities, which increases the production capacity per unit. This in turn means lower capital cost outlay and reduced footprint when building new plants
- It allows plating from more dilute electrolyte. This is especially useful for removing toxic/harmful metals from waste streams and the recovery of precious metals from process streams.
-

Various cell designs have been developed to improve mass transfer (Marshall 1985) (Cooper 1985):

- Packed Bed Reactor
- Air agitation in cells
- Fluidized Bed Reactor
- Rotating cylinder cathode
- Annular or Cylindrical Cell

The EMEW® is an industrial application of the annular type electrochemical cell and was developed by Electrometals Technologies Limited.

Various studies in mass transfer in annular electrochemical cells have been conducted in the past using potentiometric methods. Previous workers have found that the angle, as well as the direction of swirl flow in tubular or annular cells, has an effect on the mass transfer (Martemianov 2002). Studies have also shown that mass transfer in annular cells may be increased by reducing the diameter of the cell towards the end form a conical shaped cell (Noui-Mehidi, 1999). It has been found that swirl flow in generated higher values of the friction factors and a lengthening of the entrance length and momentum transfer when compared to axial flow at the same volumetric flow rate (Legrand, 1991). Swirl flow has been found to increase mass transfer up to 400% compared to that of fully developed axial flow for the same flow rates. (Legentilhomme, 1990).

Theoretical

An electrochemical technique is used where a noble tracer element, Ag, is used to determine mass transport properties such as the mass transfer coefficient and Nernst diffusion layer thickness during electroplating from Cu electrolyte (Ettel 1974). Ag is co-deposited during the plating of copper at its mass transfer controlled rate, due to its standard potential being 460mV higher than Cu^{+2}; while Cu is plated under current controlled conditions. By determining the mass of Ag plated per unit area and time and analysing the bulk concentration of Ag in solution, the mass transfer coefficient and Nernst diffusion layer thickness can be determined:

$$i_{L,Ag} = m_{Ag}.n.F/Mr_{Ag}.t \qquad (1)$$

$$CD_{Ag} = i_{L,Ag}/A \qquad (2)$$

$$k_{L,Ag} = CD/(C_{bulk,Ag}.F) \qquad (3)$$

$$\delta_{N,Ag} = D/k_{L,Ag} \qquad (4)$$

where:

$i_{L,Ag}$ = limiting current for Ag
n = molar number
F = Faraday's constant
Mr_{Ag} = molar mass of Ag
t = time
CD = current density for Ag
A = cathode area
$k_{L,Ag}$ = mass transfer coefficient
$C_{bulk,Ag}$ = bulk concentration of Ag
$\delta_{N,Ag}$ = Nernst diffusion layer thickness for Ag
D = diffusion coefficient

The method works well under conditions where the bulk concentration of Ag can be assumed to be constant. However, due to the batch recycle system used to conduct the experiments and the tubular nature of the cell, the bulk concentration of Ag in electrolyte can not be assumed to be constant. Transient mass transfer coefficient for the entire cell may be obtained by fitting equation 5 to the Ag concentration versus time plot:

$$C_{t,Ag} = C_{i,Ag} \exp(-v.E.t/V) \qquad (5)$$

where:

$C_{t,Ag}$ = time dependant Ag bulk concentration
$C_{i,Ag}$ = initial Ag bulk concentration
v = electrolyte volumetric flow rate
E = single pass reduction extraction of Ag
V = total electrolyte volume

For the annular electrochemical cell Ag is depleted from the bulk solution as it flows upwards through the cell and the bulk concentration of the Ag in electrolyte is therefore a function of height. The annular electrochemical cell is assumed to behave as a plug flow reactor. Electroplating under mass transfer limited conditions is a first order reaction and the design equation for first order reaction in a plug flow reactor can be used to determine the bulk concentration of Ag as a function of height through the electrochemical cell:

$$C_{h,Ag} = C_{0,\ Ag} \exp(-kV_h/v) \qquad (6)$$

where:

$C_{h,Ag}$ = height dependant bulk concentration of Ag
$C_{ih,\ Ag}$ = bulk concentration of Ag at bottom of cell
k = reaction rate constant for 1^{st} order plating in cell
v = electrolyte volumetric flow rate

By combining equations 5 and 6 the bulk concentration can be determined as a function of height and time. The local mass transfer coefficient for at any point on the cathode in the cell is then calculated by using the average bulk Ag concentration for the duration of the plating and for the specific height of the section under consideration, with equations 1 through 3.

EXPERIMENTAL

The experiments were conducted using a batch re-cycle system. A 20-litre tank was used as the recycle tank. This ensured a large enough volume to keep the assumption in the batch recycle equation (5B) valid. The tank was covered to minimize heat loss and evaporation. The tank was regularly topped up with de-mineralised water to maintain the starting volume.

The tank was heated with a heating coil, fed by a heated water bath, to maintain a constant electrolyte temperature of 45^{o}C. The recycle tank was fitted with an overhead stirrer to ensure good quality mixing and heat transfer form the heating coil.

The recycle flow and feed to the annular cell was achieved with a magnetic drive centrifugal pump, which ensure consistent flow. Flow rate was controlled through a manual control valve.

The outer shell of the annular cylindrical electrochemical cell formed the cathode of the cell and the inner core of the cell the anode. A stainless steel sheath fitted against the inside of the shell served as the starter sheet for the cathodic deposits. The feed inlet to the cell could be set up tangentially or perpendicularly at the bottom of the cell. The cell discharge was fixed tangentially. The cell feed arrangement is shown in Figure 2.

Current was provided by a 0-30A DC power source, with accurate control to ±0.01A. All experiments were run under current control at 250A/m^2. The experimental setup is shown in Figure 1.

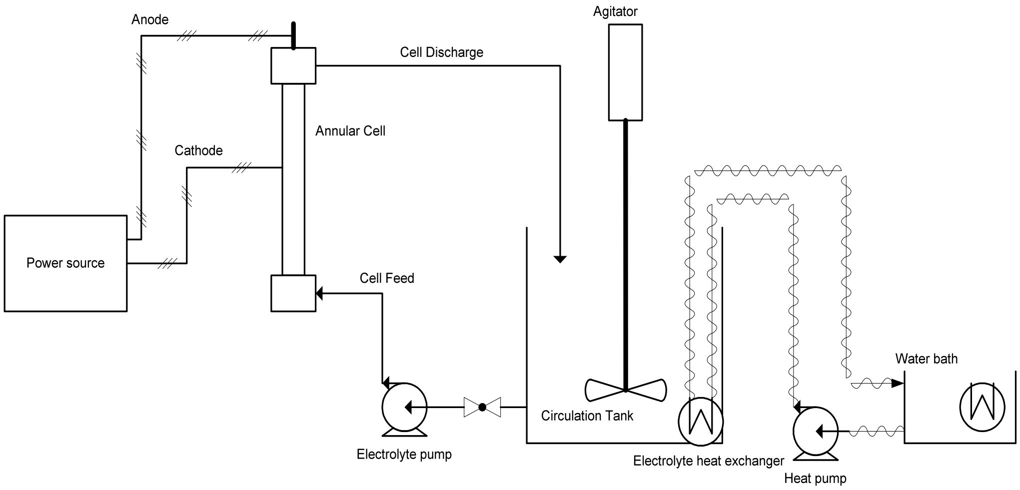

Figure 1: Experimental Setup

The stainless steels starter sheet was cleaned with HNO_3 and acetone to remove any traces of Cu, Ag and oily/organic residue, before being inserted in the cell. Electrolyte was made up in the recirculation tank to 20g/l Cu and 100g/l H_2SO_4. Only demineralised water and AR grade H_2SO_4 and $CuSO_4.5H_2O$ were used. The electrolyte was brought up to a temperature of 45^oC. Circulation was then started and current turned on to commence plating of Cu. After 3 hours circulation and current were temporarily halted to add 0.1M $AgNO_3$ in order to bring the electrolyte Ag tenor to 16mg/l. Circulation and plating were then resumed. This was done to prevent the initial plating of fine Ag powder on the stainless steel starter sheet. In initial tests were this was not done, Cu deposition was hindered by the presence of fine Ag powder on the surface of the starter sheet and very flimsy/porous deposits were obtained.

Samples were taken at regular intervals from the feed (circulation tank) and discharge of the cell (1st 3 samples) to establish the delta Cu and Ag over the cell and to determine the time dependence of the tenors in the system. The time dependence of the Ag concentration would be used to calculate the bulk mass transfer coefficient of the mass transfer limited batch recycle system. Plating continued for a period calculated to achieve ~100g of Cu deposit (average of 96% Current Efficiency). At this point the circulation and current were stopped. The cell was then drained and carefully flushed to avoid dislodging any fine granular Ag deposits on the cathode. The cell was then dismantled and the starter sheet, together with the Cu deposit, was then removed from the cell. The Cu cathode was then cut open and rolled flat. A 10x15 grid was measured and marked out. The cathode was then cut up and each of the segments weighed and analysed for their Ag content, which was then used to determine local mass transfer coefficients.

During the tests the only parameters that were varied were the flow rate through the cell and the inlet geometry. The inlet could be set up tangentially at the bottom of the cell to induce swirl flow, or perpendicularly to induce axial flow. The cell discharge from the top of the cell was tangential in all cases.

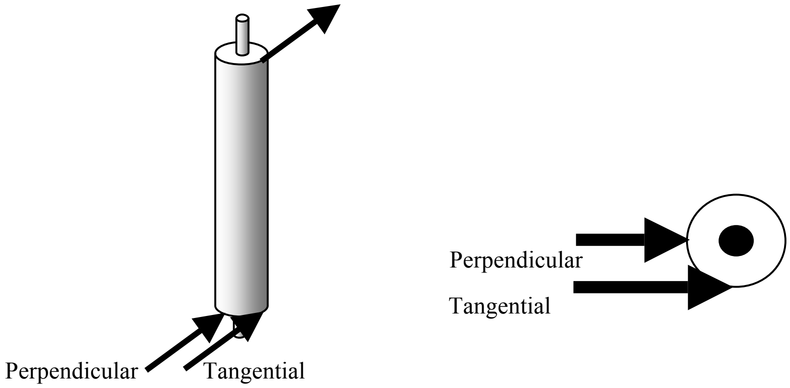

Figure 2: Annular Cell Inlet Geometry

RESULTS

The results of the Ag analysis on the cathode segments were used to calculate the local mass transfer coefficients through the cell and then plotted as contour plots to visualise the mass transfer effects and flow patterns. The results are given in Table 1. From Table 1 it can be seen that the average mass transfer coefficients for swirl flow generated by the tangential inlet is 215%, 308% and 393% higher than that obtained by the axial which is generated by the perpendicular inlet. This is in good accordance to previous findings (Legentilhomme, 1990).

The local mass transfer coefficients are plotted as contour plots to illustrate the flow patterns and mass transfer intensities through the annular electrochemical cell. The plots are grouped together for swirl flow and for axial flow at the three flow rates tested and are all plotted on the same scale. The plots depict the local mass transfer coefficients on the cathode after it was removed, cut open and rolled flat. The decaying swirl flow patterns induced by the tangential inlet are clearly discernable in the contour plots. It can also be intuitively seen that the swirl flow decays to axial flow at the lowest flow rate tested and that the axial flow induced by the tangential inlet generates lower overall mass transfer than the swirl flow. At high flow rates the perpendicular inlet causes high mass transfer at the inlet, but it can be seen that it drops of rapidly as the flow moves up the cell.

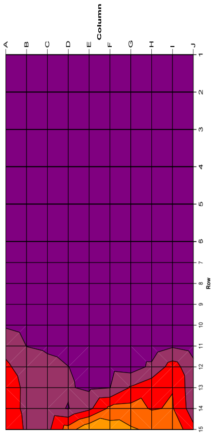

Figure 3: Tangential Inlet, Low Flow

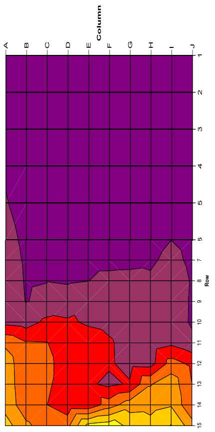

Figure 3: Tangential Inlet, Medium Flow

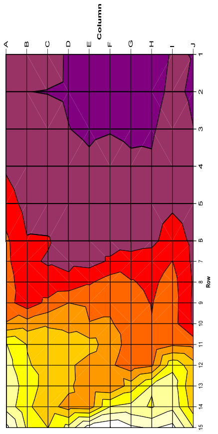

Figure 5: Tangential Inlet, High Flow

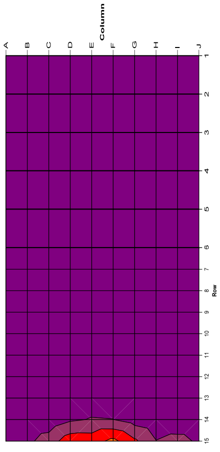

Figure 6: Perpendicular Inlet, Low Flow

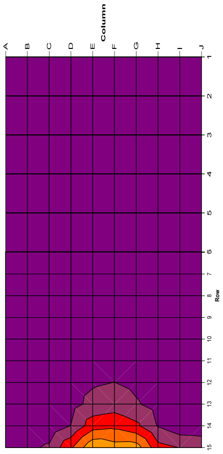

Figure 4: Perpendicular Inlet, Medium Flow

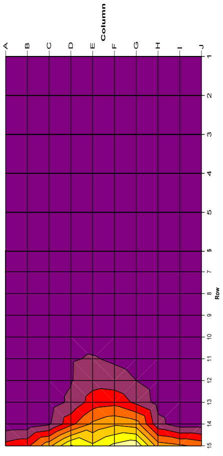

Figure 8: Perpendicular Inlet, High Flow

Table 1: Experimental Results

Test No.	Inlet Geometry	Superficial Flow Rate (cm/s)	Max k_L (cm x 10^{-3})	Min k_L (cm x 10^{-3})	Ave k_L (cm x 10^{-3})	Average δ_{Ag} (mm)
1	Perpendicular	2.37	8.15	0.29	1.00	0.28
2	Tangential	2.37	12.22	0.42	2.15	0.20
3	Perpendicular	3.75	12.15	0.42	1.37	0.24
4	Tangential	3.75	16.39	0.84	4.22	0.09
5	Perpendicular	4.45	19.46	0.51	2.14	0.20
6	Tangential	4.45	25.94	1.66	8.40	0.04

The differences in mass transfer achieved by the two different inlet geometries are further clarified by plotting the average mass transfer at various heights through the cell (Figures 9 and 10). It can be seen that even at the highest flow rate the axial flow induced by the perpendicular inlet quickly forms a diffusion layer and the mass transfer coefficients drop off to the same values obtained for the lowest flow rate (~0.0008cm/s). The mass transfer coefficients for swirl flow at the lowest flow rate decayed to the same end value obtained in the axial flow tests. This is seen as an indication of the decay of the swirl flow pattern to axial flow. At higher flow rates the mass transfer remains higher further up the cell and is an indication of the swirl flow pattern reaching further up the cell. At the highest flow rate the swirl pattern reaches all the way to the top of the cell although it is starting to decay.

For the swirl flow at the lowest flow rate and the three axial flow cases, a slight increase in mass transfer can be noted towards the top of the cell. This may be attributed to swirl flow formation starting to form as the solution nears the tangential outlet of the cell. This phenomenon is better visualised by plotting the diffusion layer thickness as a function of height, as shown in figures 11 and 12. At high flow rates this phenomena tends to be masked by the general higher mass transfer through the cell. The “bumps” in the swirl flow plots are the result of the roping swirl flow action and the resulting increased mass transfer.

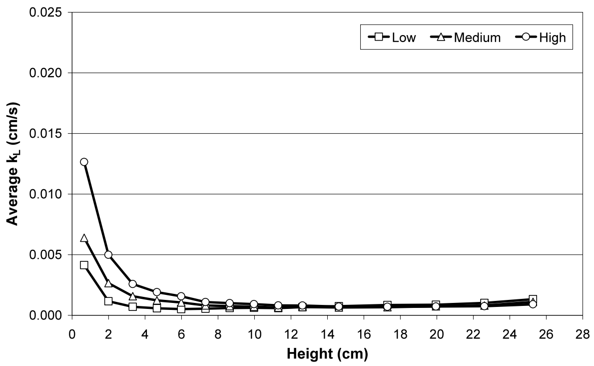

Figure 6: Mass Transfer as a Function of Height - Axial Flow

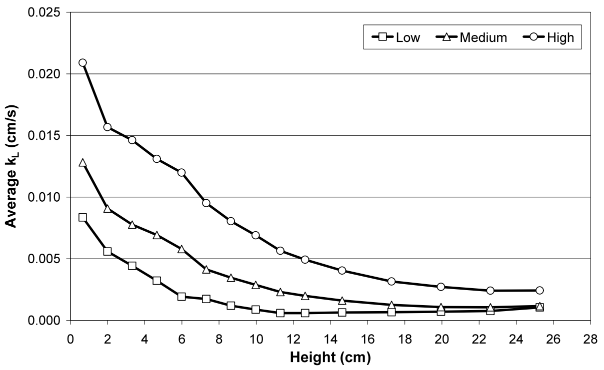

Figure 5: Mass Transfer as a function of Height - Swirl Flow

Figures 11 and 12 show how the diffusion layer thickness increases up through the height of the cell. The axial flow diffusion thickness increase rapidly at all flow rates and then decreases as it nears the tangential outlet of the cell, due to onset of swirl flow formation. The diffusion layer thickness profile for the tangential inlet at the lowest flow rate shows similar characteristics to that of the three axial flow profiles. This is due to the decay of the swirl flow to axial flow in the first half of the cell, and the onset of swirl formation close to the outlet at the top of the cell.

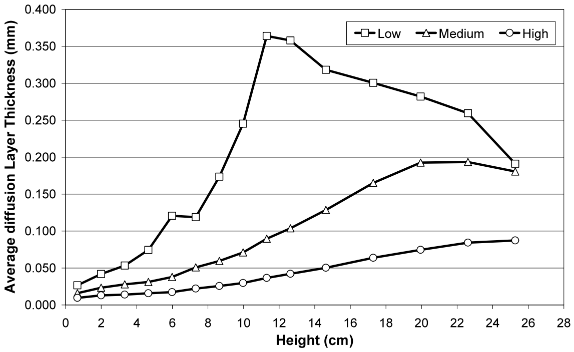

Figure 7: Diffusion Layer Thickness as a Function of Height - Swirl Flow

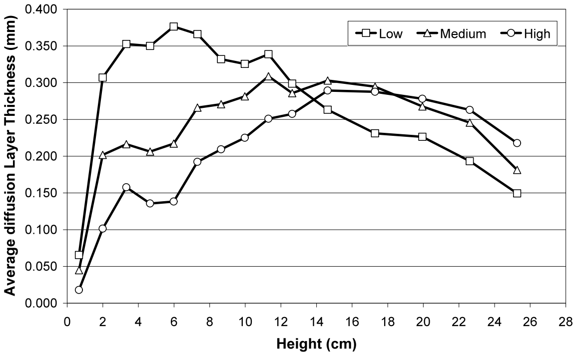

Figure 8: Diffusion Layer Thickness as a Function of Height - Axial Flow

The effect of flow rate on the average diffusion layer thickness is more marked for swirl flow than for axial flow, as shown by the slopes for the two cases in Figure 13. Linear fits to the data points converge at ~0.35mm when extrapolated to 0 cm/s superficial velocity. This compares well to the value 0.3mm, obtained by Ettel et al. (Ettel 1975) during similar test work on conventional cells with similar electrolyte, for the lower half of a vertical plate electrode under natural convection where there is very little agitation. The maximum diffusion layer thickness obtained for the lowest flow rates for both the tangential inlet and perpendicular inlet cases are also close to the 0.35mm value, which suggests that for a long annular cell at low flow rates, the mass transfer would approach that obtained by natural convection in the cell. When the tangential component of the swirl flow is brought into consideration a linear relationship is obtained between linear velocity and the average diffusion layer thickness through the cell shown in Figure 14.

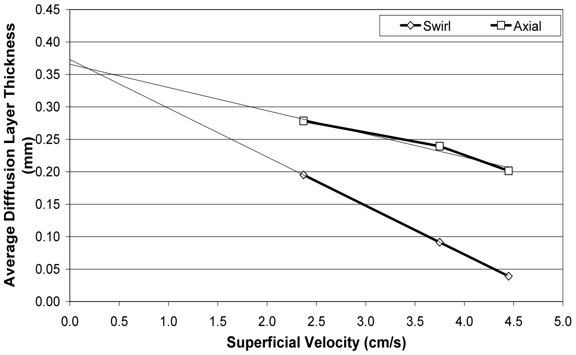

Figure 13: Average Diffusion Layer Thickness as a Function of Flow

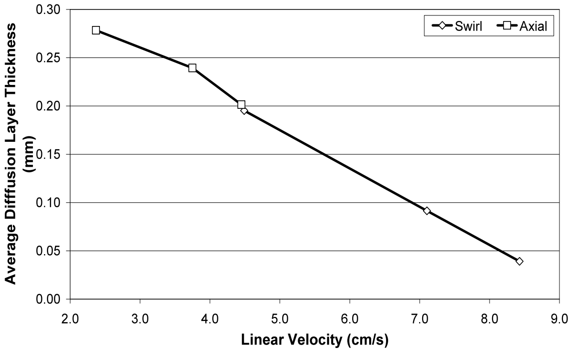

Figure 14: Average Diffusion Layer Thickness as a Function of Linear Velocity

The effect of flow rate on mass transfer is much more pronounced for tangential inlet/swirl flow than for perpendicular inlet/axial flow. This can be seen from the sharp slope and increase in slope for the average mass transfer coefficient in Figure 15. The swirl flow induced by the tangential inlet extends further up the cell at higher flows and ensures higher average mass transfer coefficients. The higher linear flow rate and the turbulence caused by the swirl flow ensure that the diffusion layer forms much slower and remains thinner through the height of the cell.

For the three perpendicular inlet cases the increase in flow rate does not significantly influence the mass transfer due to the rapid formation of the diffusion layer.

For the perpendicular inlet which induces axial flow, the local mass transfer coefficients at the inlet increase at a similar rate as the tangential/ axial inlet area with an increase in flow rate. But the diffusion layer forms much quicker and the mass transfer coefficients drop of rapidly as the flow moves further away from the inlet to values of ~0.0008 cm/s.

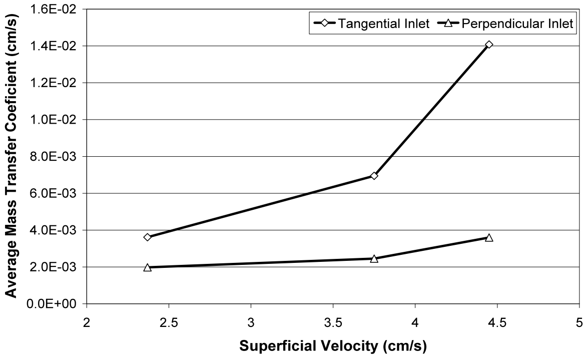

Figure 15: Average Mass Transfer as a Function of Flow

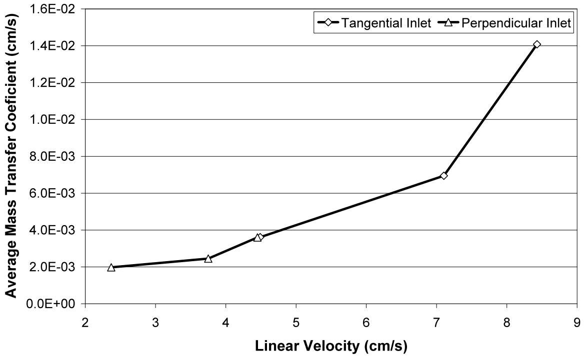

Figure 16: Average Mass Transfer as a Function of Linear Velocity

Figure 16 shows the effect of linear flow rate, when the tangential vector is factored in for swirl flow, on the average mass transfer through cell. The angle of the swirl flow was constant at 31.9°. This tangential vector meant that the actual linear flow rate for the tangential inlet was 1.9 times that of the axial flow for the same volumetric flow rates. This would suggest that for the cell dimensions tested, double the volumetric flow rate would be needed to achieve the same overall mass transfer for axial flow as for the swirl flow. In practice this would mean that achieving the same mass transfer for axial as for swirl flow would carry much higher pumping costs in an industrial application.

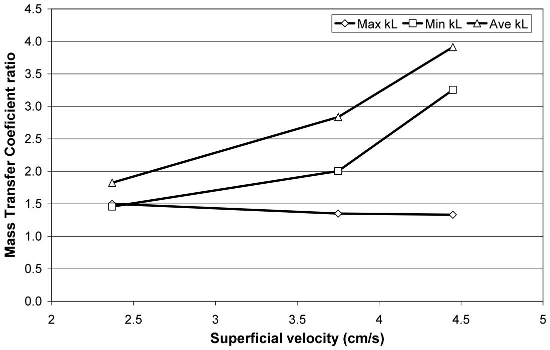

Figure 9: Swirl to Axial flow Mass Transfer Ratios as a Function of Flow

Figure 17 shows the ratio of mass transfer for swirl flow to that of axial flow, at the same flow rate. From it can be seen that the maximum mass transfer coefficients are similar for the two flow regimes and the difference decreases as the flow increases. The maximum mass transfer values are found at the inlet and are similar due to the high amount of turbulence found at the inlet region.

For the minimum mass transfer coefficient, and therefore the average as well, the difference between the swirl flow and axial flow increases as the flow rate increases. This is another clear indication of how the swirl flow pattern extends further down the cell at higher flow rates and how the turbulence caused by the swirl flow enhances mass transfer.

CONCLUSIONS

The method of using a more noble tracer metal for co-deposition during electrolytic plating (Ettel 1974, 1975), first used by Ettel et al., works very well in this application and produces direct evidence of the mass transfer characteristics in an annular electrochemical cell. The grid size used for the cathode analysis needs to be adjusted in terms of the resolution required, the available budget for analysis and the available time span. The grid size can also be made finer in areas of greater interest, as was done in this test work. From a design point of view, horizontal bands in stead of a grid may be used if the flow pattern has already been established, in order to size cells for a specific application. This method would work well in conjunction with computational flow dynamic design methods, as a final confirmation of design parameters.

The results obtained from the test work provide concrete proof that the tangential inlet generates swirl flow and that the perpendicular inlet generates axial flow in the annular cylindrical cell. Swirl flow ensures better mass transfer than axial flow at the same volumetric flow rate for a given annular cylindrical electrochemical cell. This is due in part to the higher linear velocity that the tangential vector of the flow pattern imparts to the flow. The swirl flow pattern also has a radial acceleration vector due to the cylindrical shape of the cell which forces the flow to curve along the inside of the cylinder. This causes the flow to constantly impinge on the surface of the cathode at a slight angle. The impinging flow causes turbulence and impedes the formation of the diffusion layer, which in turn brings about better mass transfer (Figure 18). The drag caused by the impinging flow slows down the flow and the swirl flow pattern remains only as long as the electrolyte maintains enough momentum. As the flow slows down it is forced to move in a more axial direction. This reduces the radial acceleration vector and allows the diffusion layer to grow thicker, which reduce mass transfer.

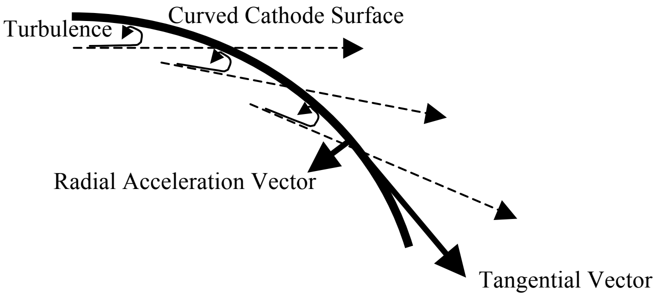

Figure 10: The Impinging Effect of Swirl Flow

Mass transfer was shown to increase with increasing flow rate. This relationship is stronger for swirl flow than for axial flow in the annular cell.

In industrial applications it would be preferable to operate cells in the regions of highest mass transfer, in order to make use of the higher limiting currents which allow much higher specific production capacities. For that reason cells with shorter aspect ratios would be preferred. Further modifications to the standard annular cell could also be considered such as the tapered annular cell (Noui-Mehidi 1999) which would enhance swirl flow due to acceleration of the solution caused by the decreasing diameter of the cell.

ACKNOWLEDGMENTS

The author would like to thank Skorpion Zinc of Anglo Base Metals, a subsidiary of Anglo operations Ltd., for making available laboratory space and funds to complete the test work. Thanks to Electrometals Canada Inc for providing the annular cylindrical electrochemical cell which was used to conduct the tests. Thanks to De Bruyn Spectroscopic Solutions for performing the analysis on the electrolyte and cathode sections. Thanks to David Dreisinger form the University of British Colombia for his advice. Special thanks to Mike Nicol from Murdoch University for providing guidance, advice and reviewing the paper.

BIBLIOGRAPHY

Ettel,V.A., Tilak, B.V., Gendron, A.S. 1974. Measurement of Cathode Mass Transfer Coefficients in Electrowinning Cells. Journal of Electrochemical Society: Electrochemical Science and Technology, 121(7): 867-872

Ettel, V.A., Gendron, A.S. 1975. The Role of Mass Transfer in Designing Electrowinning Cells. Chemistry and Industry, 3 May 1975 : 376-377

Ettel, V.A., Gendron, A.S., Tilak, B.V. 1975. Electrowinning Copper at High Current Densities. Metallurgical Transactions B, 6B(?): 31-36 Reference

Gendron, A.S., Ettel, V.A., 1975. Hydrodynamic Studies in natural and Forced Convection Electrowinning Cells. The Canadian Journal of Chemical Engineering, 53(?) : 36-40

Wang, H.M., Chen, S.F., O'Keefe, T.J., Degrez, M., Winand, R. 1989. Evaluation of Mass Transport in Copper and Zinc Electrodeposition using Tracer Methods. Journal of Applied Electrochemistry, 19(?) : 174-182

Noui-Mehidi, M.N., Salem, A., Legentilhomme, P., Legrand, J. 1999. Overall Mass Transfer in the Swirling Flow induced by a Tangential Inlet between Coaxial Cones. Journal of Applied Electrochemistry, 29(?): 1277-1284

Aouabed, H., Legentilhomme, P., Nouar, C., Legrand, J. 1994. Experimental Comparison of Electrochemical and dot-Paint Methods for the Study of Decaying Swirling Flow. Journal of Applied Electrochemistry, 24(?): 619-625

Legrand, J., Legentilhomme, P, Aouabed, H., Ould-Rouis, M., Nouar, C., Salem, A. 1991. Electrodiffusional Determination of the Momentum Transfer in Annular flows: Axial developing and Swirling Decaying Flows. Journal of Applied Electrochemistry, 21(?): 1063-1067

Legentilhomme, P., Legrand, J. 1990. Overall Mass Transfer in Swirling Decaying Flow in Annular Electrochemical Cells. Journal of Applied Electrochemistry, 20 (?) : 216-222

Martemianov, S., Okulov, V.L. 2002. Mass Transfer Ambiguities in Swirling Pipe Flows. Journal of Applied Electrochemistry, 32(?): 25-34

Yapici, S., Partrick, M.A., Wragg, A.A. 1995. Electrochemical Study of Mass Transfer in Decaying Annular swirl Flow, Part 2: Correlation of Mass Transfer Data. Journal of Applied Electrochemistry, 25(?): 15-22

Yapici, S., Patrick, M.A., Wragg, A.A. 1994. Electrochemical Study of Mass Transfer in Decaying annular Swirl Flow, Part 1: Axial Distribution of Local Mass Transfer Coefficients. Journal of Applied Electrochemistry, 24(?): 685-693

Ross, T.K., Wragg, A.A. 1965. Electrochemical Mass Transfer Studies in Annuli. Electrochemica Acta, 10(?) : 1093-1106

Cooper, W.C. 1985. Advances and Future Prospects in Copper Electrowinning, Journal of Applied Electrochemistry, 15(?): 789-805

Marshall, R.J., Walsh, F.C. 1985. Surface Technology, 24(?) : 45-77

Picket, D.J. 1973. The Analysis of a Batch Electrochemical Reactor with Continuously Recirculating Electrolyte. Electrochemica Acta, 18(?) : 835-837